Nature Environment and Pollution Technology
An International Quarterly Scientific Journal

p-ISSN: 0972-6268
(Print copies up to 2016)
e-ISSN: 2395-3454

Vol. 23 | No. 1 | pp. 365-379 | 2024

Original Research Paper

https://doi.org/10.46488/NEPT.2024.v23i01.031

Open Access Journal

Mapping and Monitoring of Land Use/Land Cover Transformation Using Geospatial Techniques in Varanasi City Development Region, India

Atul K. Tiwari, Anindita Pal† and Rolee Kanchan

Department of Geography, Faculty of Science, The Maharaja Sayajirao University of Baroda, Vadodara-390002 Gujarat, India

†Corresponding author: Anindita Pal; anindita.geogphd@msubaroda.ac.in

Nat. Env. & Poll. Tech.
Website: www.neptjournal.com

Received: 14-07-2023
Revised: 22-08-2023
Accepted: 21-09-2023

Key Words:
Google Earth Engine
Landsat-9
Machine learning
Random forest classifier
Land use/Land cover

ABSTRACT

Assessing the dynamics and patterns of Land Use and Land Cover (LULC) and its transformation is an important practice of urban planners and environmentalists for a variety of applications, including land management, urban climate modeling, and sustainability of any urban region. Monitoring changes in LULC using geospatial techniques can help to identify areas at risk for indefensible land use, low-grade environment, and especially for sustainable urban planning. This study aims to analyze the changing pattern, dynamics, and alteration of LULC using Google Earth Engine (GEE) and Machine Learning Applications for the years 1991, 2001, 2011, and 2022 in the Varanasi City Development Region (VCDR). The LULC classification was divided into seven classes using random forest classification, and Landsat-5(TM) and 9(OLI-2) satellite data were used. Saga GIS has been utilized for the detection of LULC change during the 1991-2022 period. For validation of classification results, accuracy assessment was estimated using error matrices and through user, producer, and overall accuracy estimation. The Kappa statistics were applied for the reliability of the accuracy assessment result. As a result, the built-up area increased by 507.8 percent, and other classes like agricultural, barren, fallow land, and vegetation cover rapidly declined and altered into concrete areas over the period. Water bodies and river sand classes have been slightly converted into different classes. The finding explains that 114.8 km^2 of fertile agricultural land, 14.81 km^2 barren land, and 12.93 km^2 of vegetation cover transformed into impervious surface, which is unsustainable and causes various problems like food scarcity, environmental degradation, and low quality of urban life. This study can be a useful guide for urban planners, academicians, and policymakers by providing a scientific background for sustainable urban planning and management of VCDR and other cities as well.

INTRODUCTION

The phenomenon of Earth's land cover has changed over the last two centuries, which has been triggered by economic development and population growth (Hu & Hu,2019). Furthermore, it is expected that the pace of these changes will continue to accelerate in the coming years (Geng et al. 2023, Pande 2022, Saravanan & Abijith 2022). The changes that are occurring at a rapid pace are overlaid on top of long-term climate dynamics and scarcity of natural resources (Pandey et al. 2021). The ability of the land to sustain human activities through the provision of multiple ecosystem services is affected by land cover change, and the resultant economic activities cause feedback that affects climate and other facets of global change (Tyagi et al. 2023). Consequently, systematic assessments of Earth's land cover must be conducted at a frequency that allows for the monitoring of both long-term trends and inter-annual or decadal variability (Chandole & Joshi 2023). Moreover, these assessments must be performed at a level of spatial and temporal specificity that permits the examination of human-driven changes (Pal et al. 2023).

Land Use and Land Cover (LULC) refers to all the living and non-living components that are present on the surface of the Earth and are considered to be one of the most critical assets of the Earth system (Chughtai et al. 2021). Its importance stems from three fundamental ways. First of all, land use interacts with the atmosphere, regulating the hydrological cycle and maintaining the energy budget, which is essential for predicting weather and climate. Secondly, it plays a significant role in the carbon cycle, acting as both a source and sink of carbon (Arévalo et al. 2020). Last but not least, land cover reflects the availability of resources such as food, fuel, timber, fiber, and shelter for human beings. It serves as a crucial indicator of other ecosystem services,

such as biodiversity (Osman et al. 2018). The information on land use is vital for many regional (Wagh 2022) and global applications, especially urban land use (Shukla & Jain 2019). To manage and maintain these valuable resources, it is crucial to understand the dynamics of LULC Changes (MohanRajan et al. 2020). With the help of advanced remote sensing technologies, it is now possible to monitor these changes at various scales and provide valuable information for policymakers and academicians (Mishra et al. 2020).

The study of LULC is scholarly important for several reasons, such as sustainable land use practices, protecting ecosystems, mitigating climate change (Sobha & Jose 2023), and promoting the well-being of both humans and the environment of any urban space (Tiware 2014). Hence, the study of patterns and dynamics of LULC in the Varanasi City Development Region (VCDR) is an attractive field of study due to its historical, geographical, and economic importance. The intricate interplay between the forces that shape the utilization and coverage of land is a fascinating phenomenon that requires attention. It is a multifaceted issue that necessitates a subtle comprehension of the factors that influence how land is used and how it evolves over space and time. The objectives of the study are to analyze the trend and pattern of LULC using Google Earth Engine (GEE) and Machine Learning Approach and assess the land transformation during the period in the study area. This study presents a juncture to acquire insights into the complicated pattern of land use and its transformation for the years 1991, 2001, 2011, and 2022.

STUDY AREA

According to Mark Twain, "Benares is older than history, older than tradition, older than legend, and looks twice as old as all of them put together." Varanasi City (Kashi/Benares/Banaras) is one of the oldest settlements in the world and it lies between rivers Varuna and Assi. The Varanasi City Development Region (VCDR) is located between 25º08'01"N to 25º28'35"N and 83º10'17"E to 82º51'04"E. The total geographical area is 67334.22 hectares (Master Plan-2031). The average elevation is 77 m from the mean sea level, but it varies in different parts. The average annual rainfall and temperature are 1067 mm and 33.4ºC respectively. April is the driest and August is the wettest month in the region. The total population of VCDR was around 2.5 million in 2011 and is estimated at 3.36 million in 2021 by the Varanasi Development Authority (VDA). The sex ratio was 887 females/1000 males, and the literacy rate was around 80 percent. The region is one of the fast-growing urban regions of Gangetic Plain due to some major service centers like Shri Kashi Vishwanath Temple, Banaras Hindu University (BHU), Banaras Locomotive Works (BLW), Sarnath Archaeological Sites, Cantonment and Lal Bahadur Shastri International Airport. The planning of the

Table 1: Specification of the Used Satellite Data.

Satellite/Sensor	Landsat-5(TM)	Landsat-9(OLI-2)
Provider	USGS	
Spatial Resolution	30 metre	
Radiometric Resolution	8 bit	12 bit
Spectral Resolution	0.45-2.35(µm)	0.43-12.51
Acquisition Date	21/05/1991; 16&24/05/2001 28/05/2011	18/05/2022
Row/Path	142/042&043	142/042
Period Covered	1991, 2001 & 2011	2022

Source: http://developers.google.com/earth-engine/datasets

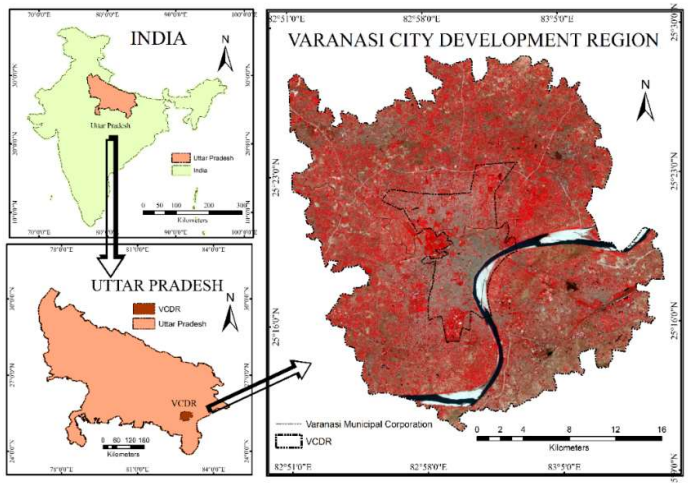

Fig. 1: Study area.

city region is the ideal approach for futuristic and sustainable development. That is the reason for choosing VCDR as the study area (Fig. 1).

MATERIALS AND METHODS

Data Sources and Tools

The LULC classification has been done using secondary data such as satellite images, Google Earth Pro temporal imageries, and prepared LULC maps of different institutions like the National Remote Sensing Centre (NRSC) and Global Land Cover data of the Environmental System Research Institute (ESRI). The primary data was also used for ground truthing and accuracy assessment, such as Global Positioning System (GPS) control points. The Landsat-5 TM and Landsat-9 OLI-2 satellite data of the United States Geological Survey (USGS) have been used for this study (Table 1). All datasets have a 30-meter spatial resolution, but the radiometric and spectral resolutions are different. The satellite data (level-1 and collection-2) was pre-georeferenced to Universal Transverse Mercator (UTM) zone 44 North projection with WGS-84 datum. The entire satellite data was processed and acquired using a custom algorithm and the GEE cloud-based platform. In this study, several tools have been used for image classification, pixel correction, accuracy assessment, finalization of maps, and graph making (Table 2).

Methodology

The significance of the methodology lies in the fact that it ensures that the study is conducted in an organized and exhaustive manner, making the results more reliable, accurate, and simple to replicate. In this study, the task-based methodology has been adopted and applied, which is outlined in Fig. 2.

LULC Classification Using Google Earth Engine

GEE is a cloud-based platform that gives users quick access to massive amounts of geographical data as well as strong analytical capabilities in the spatiotemporal context (Sudmanns et al. 2018). It facilitates scaling computations, time series data analysis, collaborative interaction, and monitoring of environmental fluctuations, etc. (Gomes et al. 2020). It is significant for its data accessibility, scalability, time-series analytic capabilities, collaborative features, conservation and environmental monitoring effect, and promotion of open data and open-source standards (Baig et al. 2022). GEE is also capable of LULC classification and is more convenient in the context of time and data acquisition (Naikoo et al. 2022). In this study, GEE has been used for LULC classification with the following steps with the help of programming in JavaScript.

Initially, the satellite data for Landsat-5 and 9 was acquired for the Area of Interest (AoI). The chosen dataset covers the years 1991, 2001, 2011, and 2022 years. The images were preprocessed using specific plugins available within the Google Earth Engine platform, which effectively eliminated the anomalies present in the satellite imagery, such as cloud cover, shadows, or atmospheric effects, through the application of image processing techniques, specifically cloud masking algorithms. Furthermore, to enhance the quality and consistency of the images, radiometric and atmospheric corrections were initiated. Layer stacking and band composition have been done and converted into a single multiband image for the particular time period. These are important processes that help in the integration of spectral information for achieving more accuracy in the classification and visualization of land features to create the training set process. A set of representative training samples has been created for learning machines to classify each of the seven LULC classes, such as built-up areas, water bodies,

Table 2: Applied Tools and Their Utilisation.

Tool	Version	Utilised For
ArcGIS	10.8	Band composition and final layout of maps
Google Earth Engine	NA	LULC classification
JavaScript	ECMAScript 2020	Programming code generation
Google Earth Pro	Multiple Temporal Images	Accuracy assessment
GPS	Garmin GPS maps 78s	GCPs collection
R-Programme	R-4.3.0	Graph making
Python	Python-3.5.3	
Saga GIS	7.8.2	LULC change detection

Source: Based on the applied tools in the study

Table 3: Description of training sets for classification.

LULC Class	Number of Polygons			
	1991	2001	2021	2022
Built-up land	95	130	129	142
Water Bodies	50	36	43	53
Agricultural land	171	96	126	138
Vegetation Cover	36	65	51	62
River Sand	37	48	19	20
Barren land	55	47	44	39
Fallow Land	54	69	61	52
Total Signatures	498	491	473	506

Source: Based on the Image Classification Process

agricultural land, barren land, fallow land, vegetation cover, and river sand within the study area frame. The training sets were prepared carefully as small polygons, and it was taken using a stratified random sampling technique (Table 3). Additionally, the existing land cover data of ESRI and NRSC were used to test and verify the prepared training samples. The Random Forest Classifier (RFC) algorithm was selected as a classification method to consider the strengths and limitations of the algorithm, such as accuracy, computational efficiency, and sensitivity.

Furthermore, prepared training sets were tested and validated the model using the validation subset to assess its accuracy and make necessary adjustments, such as fine-tuning hyperparameters. The entire stacked images were classified into seven LULC classes using a trained classification model (RFC) and generated the classified raster images (Pande 2022). The prepared raster-classified images have been extracted and post-processed using the ArcGIS 10.8 application.

Accuracy Assessment of Classification

Accuracy assessment is the most significant process for LULC classification. It is an estimation of the reliability of LULC maps. In this work, points have been created using stratified random sampling techniques and a fishnet tool to verify the classified pixels (Singh & Talwar 2013). Three types of accuracy estimation were computed, which are Overall, User, and Producer accuracy using an error matrix. The User Accuracy (UA) has been calculated using the following formula (Eq.1):

$$\alpha = \frac{n}{N} \times 100 \quad \ldots(1)$$

Where 'α' is the UA, 'n' denotes the number of corrected points classified on the image, and 'N' is the number of points verified in the field (Naikoo et al. 2022). The Producer Accuracy (PA) was measured with the help of given formula (Eq.2):

$$\beta = \frac{\sum Dij}{Rj} \quad \ldots(2)$$

Where 'β' is the PA, 'Dij' represents the corrected classified pixels in the row 'i' (diagonal cell), and 'Rj' is the total number of pixels in row 'j' (Smiraglia et al. 2016). The Overall Accuracy (OA) is the most significant accuracy type, which denotes the overall reliability of image classification (Eq.3).

$$\gamma = \frac{\sum Dij}{Cj} \quad \ldots(3)$$

Where 'γ' denotes OA, 'Dij' is the corrected & classified pixels in column j (diagonal cell), and 'Cj' is the total pixels in column 'j'. Kappa statistic is the most broadly used measurement of LULU classification accuracy to establish the relationship between two variables (Eq.4).

$$k = \frac{N\sum_{i-1}^{r} X_{ii} - \sum_{i=1}^{r}(X_{i+} \times X_{+i})}{N^2 - \sum_{i=1}^{r}(X_{i+} \times X_{+i})} \quad \ldots(4)$$

Where 'k' represents the kappa coefficient, 'N' is the total number of observations, 'r' denotes the total number of rows present in the error matrix, X_{ii} is the number of observations present in row and column 'i' respectively, X_{i+} is the total number observations in row 'i' and 'X_{+i} is the total number of observations in column 'i' (Gudex-Cross et al. 2017).

LULC Change Detection Analysis

The analysis of land use change involves assessing LULC data, which were gathered across a number of different periods to identify alterations. The change detection method contributes to an improved understanding of the repercussions of how land is exploited throughout this period (Kim 2016, Baig et al. 2022). Detecting, identifying, and estimating the changes in land use provides insights that could ultimately be used in decision-making and the creation of futuristic plans (Henits et al. 2016). Monitoring land use change through the application of Remote Sensing (RS) and GIS techniques enables an examination of spatial and temporal patterns, which helps in ensuring the oversight of land resources in a sustainable manner (Cao et al. 2022, Mahmoud et al. 2022) and in the resolution of environmental issues (Shi et al. 2021). In the beginning, the prepared classified raster dataset has been converted into a vector file. Through the implementation of the dissolve geoprocessing tool, the dataset has been amalgamated into seven distinct classes as previously outlined. Again, the intersection method was applied to detect the changes during

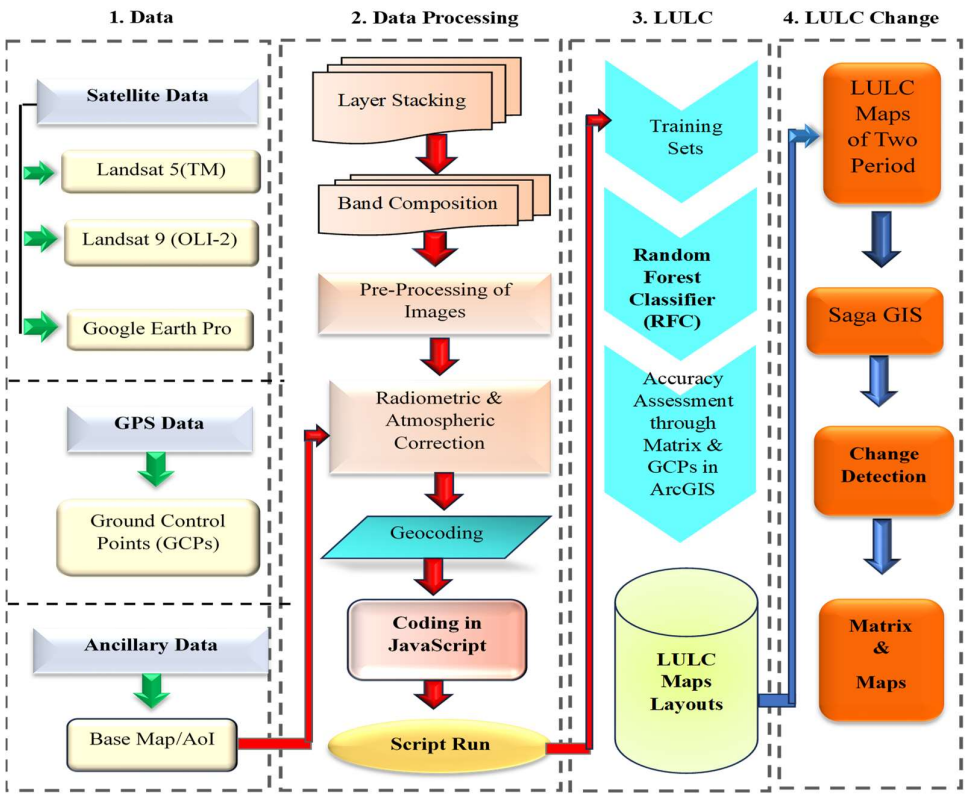

Fig. 2: Picturesque of adopted methodology.

the period classification. The transformation matrix has been exported through the Saga GIS application and plotted using R-programme for making the visual presentation of the statistics of transformed land.

RESULTS

Accuracy Assessment

The accuracy assessment is one of the most significant processes in LULC classification which helps to validate and verify the classification result. In this study, class-wise accuracy has been assessed, and the user, producer, and overall accuracy were also calculated. A total of 735 reference points have been selected through a stratified random sampling method, with 105 points in each LULC class. For estimation of the relationship between user and producer accuracy, the Kappa coefficient has been used. Table 4 presents the range of kappa coefficient values and their strength of covenant.

Accuracy Assessment in 1991

Table 5 presents the accuracy assessment matrix for 1991. Out of 735 reference points, a total of 675 points have been found correctly classified, which describes 91.83 percent of overall accuracy. Overall, above 86 percent user accuracy has been observed for each class, and producer accuracy is above 88 percent for each class. The highest user and producer accuracy were noted in the river sand and water bodies classes, respectively. The Kappa coefficient was 0.9047, which presents the strong agreement between user and producer accuracy variables and also explains the excellent classification results.

Accuracy Assessment in 2001

Table 6 corresponds to the result of the accuracy assessment for the 2001 LULC classification. Out of a total of 735

Table 4: Kappa Coefficient Range and Its Description.

k-value	Strength of Covenant
< 0.20	Strongly Disagree
0.20 - 0.40	Disagree
0.40 - 0.60	Neither Agree Nor Disagree
0.60 - 0.80	Agree
0.80 - 1.00	Strongly Agree

Source: Rwanga and Ndambuki (2017)

Table 5: Error Matrix for Accuracy Assessment of 1991 Classification.

Class	BL	WB	AL	BRL	FL	RS	VC	TU	**UA (%)**
BL	**97**	1	1	3	3	0	0	105	**92.38**
WB	0	**95**	1	0	0	7	2	105	**90.47**
AL	2	0	**94**	2	2	0	5	105	**89.52**
BRL	3	0	2	**91**	5	1	3	105	**86.66**
FL	1	0	1	5	**98**	**0**	0	105	**93.33**
RS	0	1	0	0	0	104	**0**	105	**99.04**
VC	1	0	4	1	3	0	**96**	105	91.42
TP	104	97	103	102	111	112	106	TU=735	**TC=675**
PA (%)	**93.26**	**97.93**	**91.26**	**89.21**	**88.28**	**92.85**	**90.56**		
Overall Accuracy= **91.83%**					Kappa= **0.9047**				

Source: Based on Accuracy Assessment Result of 1991

Table 6: Error Matrix for Accuracy Assessment of 2001 Classification.

Class	**BL**	**WB**	**AL**	**BRL**	**FL**	**RS**	**VC**	**TU**	**UA (%)**
BL	**93**	0	0	6	2	4	0	**105**	**88.57**
WB	0	**105**	0	0	0	0	0	**105**	**100**
AL	1	1	**93**	0	2	0	8	**105**	**88.57**
BRL	10	0	2	**79**	9	3	2	**105**	**75.23**
FL	2	0	14	6	**80**	**2**	1	**105**	**76.19**
RS	0	0	0	0	0	**105**	0	**105**	**100**
VC	1	0	9	1	3	0	**91**	**105**	**86.66**
TP	**107**	**106**	**118**	**92**	**96**	**114**	**102**	**TU=735**	**TC=646**
PA (%)	**86.91**	**99.05**	**78.81**	**85.86**	**83.33**	**92.1**	**89.21**		
Overall Accuracy= **87.89%**					Kappa= **0.8587**				

Source: Based on Accuracy Assessment Result of 2001

reference points, a total of 646 corrected points have been identified, which means the overall accuracy has been 87.89 percent. The user accuracy was 88.57, 100, 88.57, 75.23, 76.19, 100, and 86.66 percent for built-up areas, water bodies, agricultural land, barren land, fallow land, river sand, and vegetation cover, respectively. The highest and lowest producer accuracy were found in water bodies (99.05%) and agricultural land (78.81%) classes, respectively. The kappa coefficient, which was 0.8587, indicated a high level of agreement between the accuracy results of both the user and the producer, with a strong level of precision.

Accuracy Assessment in 2011

Table 7 presents the accuracy assessment result of the image classification of 2011. A total of 638 corrected points were noted, and 97 reference points were found to be incorrectly classified. The producer accuracy was observed to be 85.84, 99.03, 77.58, 86.2, 82.83, 92.1, and 84.31 percent for the built-up area, water bodies, agricultural land, barren land, fallow land, river sand, and vegetation cover, respectively. The result of user accuracy was 92.38, 98.09, 85.71, 71.42, 78.09, 100, and 81.9 percent for the built-up area, water bodies, agricultural land, barren land, fallow land, river sand, and vegetation cover, respectively. The Kappa coefficient was 0.846, which corresponds to the strong agreement between both user and producer accuracy results.

Accuracy Assessment in 2022

Table 8 presents the accuracy assessment matrix for 2022. Out of 735 reference points, a total of 682 points have been found correctly classified, which described 92.79 percent of overall accuracy. Altogether, above 83 percent user accuracy has been noted for each class, and producer accuracy was found to be above 88 percent for each class. The highest user and producer accuracy were established in the river sand and water bodies classes, respectively. The lowest has been noted in fallow land and barren land respectively. The Kappa coefficient was estimated to be 0.9158 which presented a strong covenant between user and producer accuracy variables and also explained the outstanding classification result.

Table 7: Error Matrix for Accuracy Assessment of 2011 Classification.

Class	BL	WB	AL	BRL	FL	RS	VC	TU	UA (%)
BL	**97**	0	0	1	1	6	0	105	**92.38**
WB	0	**103**	0	0	0	2	0	105	**98.09**
AL	0	0	**90**	3	5	0	7	105	**85.71**
BRL	13	1	2	**75**	10	0	4	105	**71.42**
FL	3	0	8	6	**82**	1	5	105	**78.09**
RS	0	0	0	0	0	105	0	105	**100**
VC	0	0	16	2	1	0	86	105	81.9
TP	113	104	116	87	99	114	102	TU=735	TC=638
PA (%)	85.84	99.03	77.58	86.2	82.83	**92.1**	**84.31**		
Overall Accuracy= **86.80%**					Kappa= **0.846**				

Source: Based on Accuracy Assessment Result of 2011

LULC Classification Result

In addition to an assessment of accuracy, the outcome of this study has been partitioned into various categories, including spatial patterns, dynamics, and the detection of changes in LULC. The findings were presented in a manner that corresponds to the LULC classification in chronological order.

Coverage, Trend, and Pattern of LULC

Table 9 presents summary statistics of the LULC results for the years 1991, 2001, 2011, and 2022. As per the overall result, agricultural land was found as the highest LULC class, which was 72.94, 71.36, 69.14, and 59.31 percent in 1991, 2001, 2011, and 2022, respectively. Contrarily, water body class has been observed as 1.56, 1.49, 1.34, and 1.48 percent in 1991, 2001, 2011, and 2022, respectively. The most significant LULC class, which is the built-up area, increased at a faster pace. In 1991, only 4.45 percent area was built-up class and which became 10.01 percent in 2001. In 2011, 16.44 percent area was built up, and it reached 27.05 percent in 2022. The barren land was observed as the second highest class in 1991, and it covered 7.41 percent area of VCDR. It decreased rapidly in the coming periods and was 6.24, 2.83, and 1.45 percent in 2001, 2011, and 2022 respectively. The fallow land occupied 5.19, 4.30, 3.91, and 3.83 percent of the overall geographical expanse in the years 1991, 2001, 2011, and 2022, respectively, indicating a notable decrease in it over the time period. The vegetation cover comes under the most significant LULC class for any urban area, and as a result, 6.53, 4.91, and 4.51 percent of the area was observed under the vegetation cover. It decreased from 1991 to 2011. It increased in 2022 and reached 5.08 percent (Fig. 3).

Spatial Pattern of LULC

Generally, the spatial distribution of land uses in any urban region or umland of metropolitan cities shows a homogeneous character within the city and diversified with

Table 8: Error Matrix for Accuracy Assessment of 2022 Classification.

Class	BL	WB	AL	BRL	FL	RS	VC	TU	UA (%)
BL	**100**	0	0	2	0	3	0	**105**	**95.23**
WB	0	**102**	1	0	0	2	0	**105**	**97.14**
AL	0	0	**97**	1	4	0	3	**105**	**92.38**
BRL	4	0	3	**92**	4	2	0	**105**	**87.61**
FL	1	0	2	9	**88**	0	5	**105**	**83.8**
RS	0	0	0	0	0	**105**	0	**105**	**100**
VC	0	0	6	0	1	0	**98**	**105**	**93.33**
TP	**105**	**102**	**109**	**104**	97	112	106	TU=735	TC=682
PA (%)	95.23	100	88.99	88.46	90.72	93.75	92.45		
Overall Accuracy = **92.79%**					Kappa = **0.9158**				

Source: Based on Accuracy Assessment Result of 2022

Table 9: Summary Statistics of LULC Classification.

LULC Class	1991		2001		2011		2022	
	km^2	%	km^2	%	km^2	%	km^2	%
Built-up Land	29.97	4.45	67.37	10.01	110.75	16.44	182.16	27.05
Water Bodies	10.52	1.56	10.03	1.49	9.07	1.34	10.01	1.48
Agri. Land	491.16	72.94	480.52	71.36	465.59	69.14	399.37	59.31
Barren Land	49.92	7.41	42.04	6.24	19.12	2.83	9.78	1.45
Fallow Land	34.95	5.19	28.98	4.30	26.33	3.91	25.80	3.83
River Sand	12.87	1.91	11.38	1.69	12.07	1.79	12.01	1.78
Veg. Cover	43.94	6.53	33.01	4.91	30.4	4.51	34.20	5.08

Source: Calculated based on the Classification

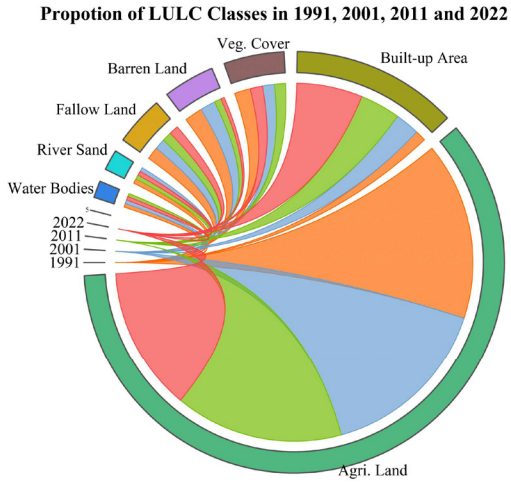

Fig. 3: Proportion of LULC Classes using Chord diagram.

a dynamic nature in the peri-urban region. Partially, the same character of dynamism can be seen in the spatial distribution of land uses in the VCDR from 1991 to 2022.

In 1991, the maximum built-up area was found within the municipal area, and some of it was observed in the southeastern part of the region. The core area and CBD were highly concentrated in the context of impervious surfaces. As a result, most of the area has been noticed under the agricultural land and it was distributed evenly in the outer parts of the city. Although, some patches of agricultural land have been identified within the municipal area. The fallow land was scattered over the region (excluding city parts), and it was more concentrated in the northern and western peripheral portions. The barren land was found in a clustered pattern, which expresses the natural causes behind it to remain barren. The largest patch of barren land was observed in the eastern part of the region and along the River Ganga. Few patches have been identified in the northern parts. Vegetation cover was found scattered, but within the city area, some areas like Banaras Hindu University, Banaras Locomotive Works, and Cantonment had dense vegetation cover.

In 2001**,** the built-up area increased and was spread over the central and southern parts of the municipal area. The leapfrog pattern of built-up land was observed in the northern parts of the city boundary. Similarly, in Pt. Deendayal Upadhyay Nagar (formerly known as Mughal Sarai) few new patches of this land use category have been noted. The extent of vegetation coverage has notably reduced in both the municipal as well as in suburban areas of the city, except for certain areas along the banks of the River Ganga, which exhibit some sporadic patches of vegetation.

In comparison to the previous period, the percentage of barren land decreased in 2001 in totality. A considerable percentage of agricultural land class has been identified. However, there was a slight decline between 1991 and 2001. Conversely, no significant alterations were observed in the remaining LULC categories, such as water bodies, fallow land, river sand, and water bodies.

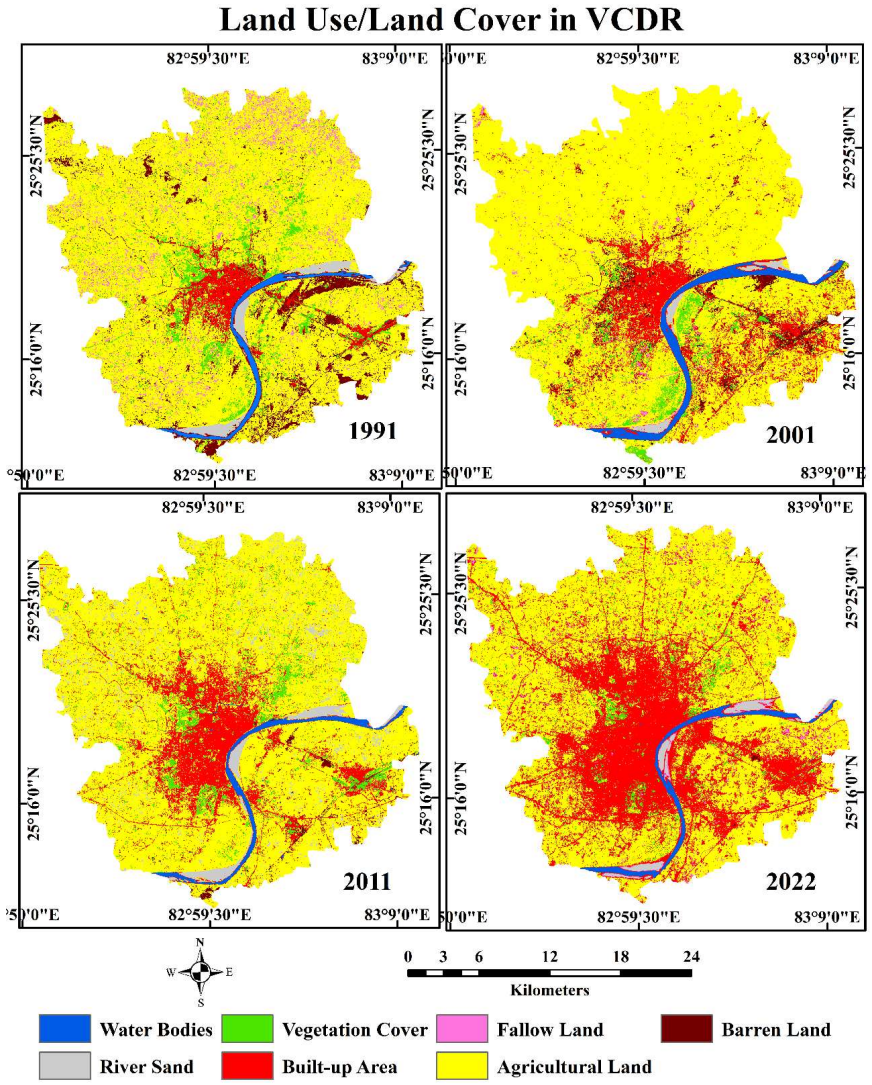

Fig. 4: Spatial distribution of Land Use/Land Cover (1991, 2001, 2011 & 2022).

During the time frame of 2011, there was a noteworthy augmentation in the built-up area along with a simultaneous and rapid escalation in density. Some new highways have been created, and the concentration of built-up areas also increased in the outer villages and towns of the study area. Again, some patches of vegetation cover have been introduced and the concentration of vegetation has increased within the municipal boundary. As a result of previous periods, the fallow, barren, and agricultural land decreased, and more spatial changes have been observed within the municipal boundary and nearer to the city boundary. The fallow and barren land class was transformed into agricultural and built-up land. No significant alterations were observed in the spatial distribution of water bodies and river sand categories.

In 2022, the built-up class has grown in the clustering pattern in the municipal area and an axial pattern in outer parts along the highways, railways, and major roads. Overall, other classes like vegetation cover, fallow, barren, and agricultural land decreased and spatially changed due to the high rate of urbanization. The water bodies and river sand have been distributed as in previous periods (Fig. 4).

Dynamics of LULC

The utilization trend and pattern of land resources can be expressed through the history and current state of a specific type of land, which is also beneficial in understanding the physical and cultural landscape dynamics in a region. In this study, land use was dynamic on a large scale. Some classes, like water bodies, vegetation cover, and river sand,

Table 10: Dynamics of LULC Classes (km^2).

LULC Class	1991-2001		2001-11		2011-22		1991-2022	
	km^2	%	km^2	%	km^2	%	km^2	%
Built-up Land	37.4	124.79	43.38	64.39	71.41	64.47	152.19	507.8
Water Bodies	-0.49	4.65	-0.96	-9.57	0.94	10.36	-0.51	-4.84
Agri. Land	-10.64	-2.16	-14.93	-3.1	-66.22	-14.22	-91.79	-18.68
Barren Land	-7.88	-15.78	-22.92	-54.51	-9.34	-48.84	-40.14	-82.41
Fallow Land	-5.97	-17.08	-2.65	-9.14	-0.53	-2.01	-9.15	-26.18
River Sand	-1.49	-11.57	0.69	-6.06	-0.06	-4.97	-0.86	-6.68
Veg. Cover	-10.93	-24.87	-2.61	-8.99	3.8	12.5	-9.74	-22.16

Sources: Calculated through the LULC classification

Table 11: Change Area Matrix of 1991-2001 (km^2).

LULC Class	Agri. Land	B. Land	Built-up	F. Land	R. Sand	Veg. Cover	W. Bodies
Agri. Land	436.21	4.9	37.21	6.11	0.48	8.46	0.94
B. Land	26.47	5.16	8.15	1.37	0.11	2.74	2.93
Built-up	0	4.36	29.97	0	0	0	0
F. Land	27.78	0.05	0.93	1.38	0.01	0.06	0.01
R. Sand	1.63	0.01	1.89	0.21	4.72	0.01	4.15
Veg. Cover	23.19	7.46	3.34	0.06	0.01	7.07	0.07
W. Bodies	3.2	0.01	0.24	0	0.05	0.04	10.18

Source: Computed through transformation result

remained the same during the time period. While, fertile land, which was either in the form of barren and fallow or agricultural land, decreased and was converted into built-up areas. Table 10 presents the dynamics of LULC for 1991-2001, 2001-11, 2011-2022, and 1991-2022 periods. The built-up area increased by 37.4, 43.38, 71.41, and 152.19 km^2 during the 1991-2001, 2001-11, 2011-2022, and 1991-2022 periods, respectively. It increased by 507.8 percent over the time period. All the other LULC classes have decreased during the study period. 18.68 percent (91.79 km^2) of agricultural land has been lost, which is a major transformation recorded in the city region. The barren and fallow land classes decreased by 82.41 and 26.18 percent, respectively, during the 1991-2022 period. In the same time period, water bodies and river sand classes have decreased by 4.84 and 6.68 percent, respectively. However, vegetation cover decreased by 24.87 and 8.99 percent in the 2001 and 2011 years, respectively. Surprisingly, it increased by 12.5 percent in the 2011 and 2022 period. Whereas, during 1991-2022, it decreased by 22.16 percent.

Change Detection and Transformation of LULC

LULC change detection refers to the process of identifying and analyzing the changes that occur in the use of land over a specific time period. It involves comparing different satellite images at different times to assess the changes in land features, including built-up areas, water bodies, barren land, fallow land, vegetation cover, and agricultural land. In this study, change detection was done to assess the land use transformation between 1991-2001, 2001-11, 2011-22, and 1991-2022.

Land Transformation During 1991-2001

Table 11 corresponds to the LULC transformation matrix for the 1991-2001 period. The most remarkable change was observed in agricultural land to a built-up area by 37.21 km^2, fallow land by 6.11 km^2, barren land by 4.9 $km^{2,}$ and vegetation cover by 8.46 km^2. 26.47 km^2 of barren land was transformed into agricultural land, built up by 8.15 km^2, fallow land by 3.37 km^2, vegetation cover by 2.74 $km^{2,}$ and water bodies by 2.93 km^2. The fallow land was converted majorly into agricultural land by 27.78 km^2. Another remarkable land use conversion has been noted in vegetation cover, which has changed 23.19 km^2 in agricultural land, 7.46 km^2 in barren land, and 3.34 km^2 in the built-up area. No changes were observed in agricultural land, barren, built-up, fallow, river sand, vegetation cover, and water bodies by 436.21, 5.16, 29.97, 1.38, 4.72, 7.07, and 10.18 km^2 area respectively (Fig. 5).

Land Transformation During 2001-2011

Table 12 presents the land use transformation during the

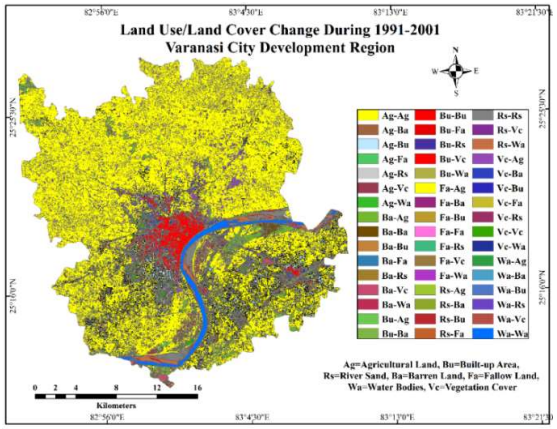

Fig. 5: LULC change detection during1991-2001.

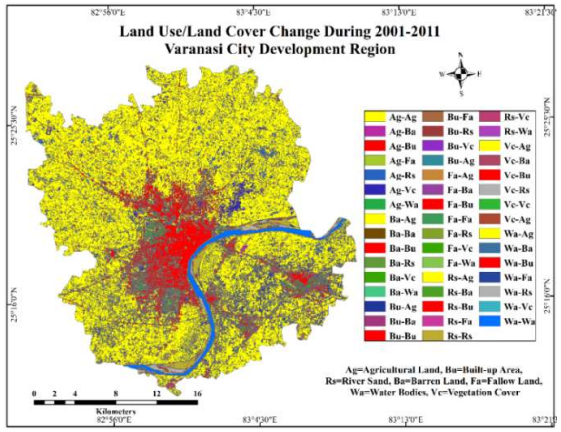

Fig. 6: LULC change Detection during 2001-2011.

2001-11 time period. As per the change detection result, no changes occurred in agricultural land, barren land, built-up area, fallow land, river sand, vegetation cover, and water bodies by 426.76, 2.07, 67.37, 0.01,4.63, 4.06, and 8.13 km^2 respectively. The major conversion was observed in agricultural land, which has transformed into barren land (2.57 km^2), built-up area (46.74 km^2), river sand (2.8 km^2), and vegetation cover (22.58 km^2). Barren land was converted into agricultural land by 12.12 km^2 and built-up area by 8.19 km^2. Whereas the built-up area was only converted into river sand and vegetation cover. Another remarkable conversion has been identified in fallow land, which has changed 8.14 km^2 area into agricultural land and 11.96 km^2 into the built-up area. Negatively, vegetation cover was converted into agricultural land by 14.98 km^2 and built-up area by 8.59 km^2. A total of 7.91 km^2 area of water bodies was transformed into agricultural land, barren land, built-up area, river sand, and vegetation cover (Fig. 6).

Land Transformation During 2011-2022

Table 13 presents the LULC transformation matrix for the 2011-2022 period. It was observed that 114.27 km^2 of agricultural land, 6.18 km^2 of fallow land, and 9.58 km^2 of vegetation cover were converted into built-up areas during the time period. The fallow land (1.01 km^2) was slightly altered into the agricultural land. Another remarkable land use conversion was identified in vegetation cover, in which 12.45 km^2 area changed into agricultural land and 11.48 km^2 into the concreted area. A total of 2.99 and 2.18 km^2 area of barren land were transformed into agricultural and built-up, respectively. The agricultural land, barren, built-up, fallow, river sand, vegetation cover, and water body classes remained by 359.9, 0.31, 110.75, 0.01, 5.98, 10.15, and 8.94 km^{2,} respectively (Fig. 7).

Land Transformation During 1991-2022

During 1991-2022, the land use was drastically altered in VCDR. In these 31 years, 114.8 km^2 of agricultural land has changed into a built-up area, and a total of 152.19 km^2 of built-up area was amplified. It altered into vegetation cover by 11.85 km^2 and fallow land by 6.31 km^2. The barren land was converted into agricultural land and built-up land by 27.5 km^2 and 14.81 km^{2,} respectively (Table 14). A total of 29.37 km^2 of fallow land was converted into agriculture,

Table 12: Change Area Matrix of 2001-11 (km^2).

LULC Class	Agri. Land	B. Land	Built-up	F. Land	R. Sand	Veg. Cover	W. Bodies
Agri. Land	426.76	2.57	46.74	0.01	2.8	22.58	0.25
B. Land	12.12	2.07	8.19	0	0.08	5.26	0.12
Built-up	0	0	67.37	0	2.11	1.95	0
F. Land	8.14	0.03	11.96	0.01	0.82	0.17	1.01
R. Sand	0.65	0.01	0.08	0.02	4.63	0.01	0.01
Veg. Cover	14.98	0.87	8.59	0	0.15	4.06	0.11
W. Bodies	2.2	0.15	1.59	0.04	3.82	0.11	8.13

Source: Computed through transformation result

Table 13: Change Area Matrix of 2011-22 (km^2).

LULC Class	Agri. Land	B. Land	Built-up	F. Land	R. Sand	Veg. Cover	W. Bodies
Agri. Land	359.9	0.02	114.27	6.18	0.34	9.58	0.77
B. Land	2.99	0.31	2.18	0.05	0.01	0.06	0.09
Built-up	0	0	110.75	0	1.18	0	0
F. Land	1.01	0	0.02	0.01	0.01	0	0.01
R. Sand	1.96	0	5.28	2.58	5.98	0.03	1.4
Veg. Cover	12.45	0.01	11.48	0.09	0	10.15	0.08
W. Bodies	0.25	0.01	1.98	0.37	0.52	0.03	8.94

Source: Computed through transformation result

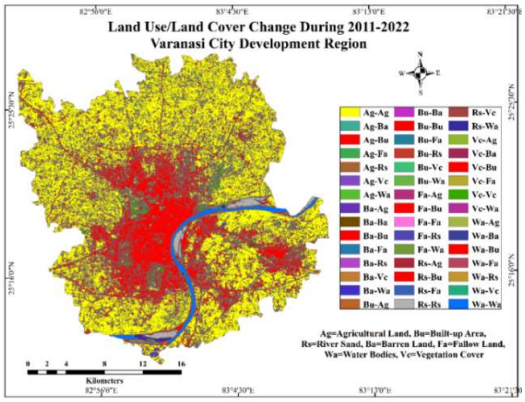

Fig. 7: LULC Change detection during 2011-2022.

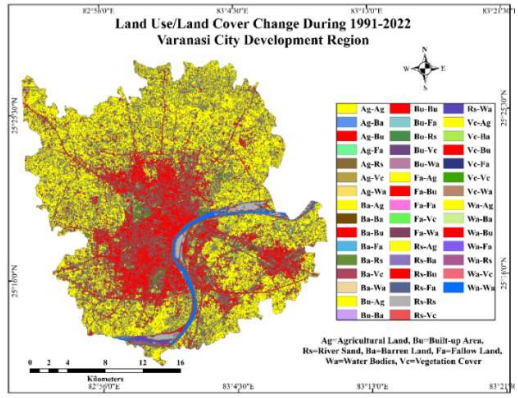

Fig. 8: LULC change detection during 1991-2022.

built-up and vegetation cover, while vegetation cover was transformed into agricultural land (4.41 km^2), barren land (3.02 km^2), and built-up area (12.93 km^2). Whereas, 374.31 km^2 agricultural land and 15.63 km^2 vegetation cover area have not been altered. Similarly, 5.81 km^2 area of river sand and 7.7 km^2 of water bodies were detected as unchanged areas (Fig. 8). Meanwhile, the built-up area class was totally unchanged due to its physical characteristics (Fig. 9).

Spatial Pattern of LULC Transformation During 1991-2022

The LULC transformation results were very interesting, but its spatial distribution was more attention-grabbing for the local governing bodies and policymakers. In the 1991-2001 period, significant changes were noted within and surrounding the municipal area. Pt. Deendayal Upadhyay Nagar town also witnessed the land alteration phenomenon.

Table 14: Change Area Matrix of 1991-2022 (km^2).

LULC Class	Agri. Land	B. Land	Built-up	F. Land	R. Sand	Veg. Cover	W. Bodies bbBBodies
Agri. Land	374.31	0.04	114.8	6.31	0.22	11.85	0.34
B. Land	27.5	0.31	14.81	0.72	0.27	0.82	1.52
Built-up	0	0	29.97	0	0	0	0
F. Land	23.53	0	5.54	0.79	0	0.3	0
R. Sand	1.07	0.01	2.41	1.14	5.81	0.01	1.17
Veg. Cover	4.41	3.02	12.93	0.21	0	15.63	0.83
W. Bodies	0.08	0.19	1.7	0.4	0.65	0.01	7.7

Source: Computed through transformation result

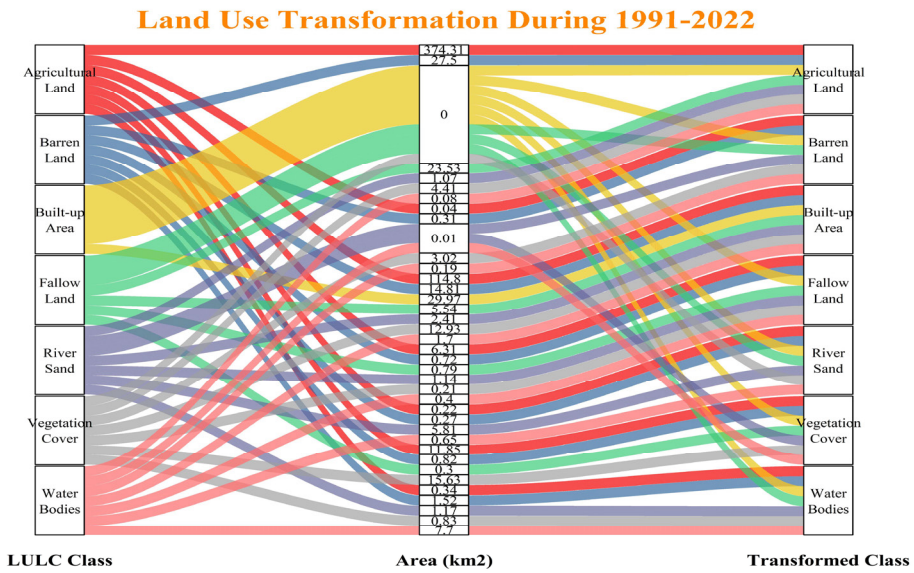

Fig. 9: Land transformation during 1991-2022 using an alluvial diagram (using Tableau and Python).

The built-up area grew at a high rate in the northern and western parts. The localities which are situated at the right bank of Ganga and Ramnagar Town, witnessed the land transformation, especially in the agricultural and barren land use classes. The LULC of peri-urban areas slightly changed into agricultural land, barren land, fallow land, and vegetation cover. In the 2001-2011 period, the axial growth pattern of LULC change was identified, which altered along the major axes like roads, railways, and river banks. The changing pattern of LULC was found towards the periphery of the study area. However, the north-central and eastern areas of the VCDR have been more dynamic than the other outer parts of the city region. In the 2011-2022 period, several urban features like highways, other major roads, railway lines, and built-up setups were constructed. Hence, massive land alteration was observed around these entities. Meanwhile, with the expansion of anthropogenic concretscapes, other land use classes have been transformed simultaneously.

DISCUSSION

According to the USGS's Department of Land Studies, accuracy should be more than 85 percent at micro-level studies, and the result of the accuracy assessment was fine on the standards. It was observed that a faster pace of urbanization is pushing to change the LULC pattern and dynamics in the city region. The agricultural land has shrunk by 18.68 percent during the 1991-2022 time period, which is paving the way for the expansion of the built-up area. This decrease is reducing the rural resources, creating imbalances in the rural economy, food scarcity, ecological degradation, etc. In the study area, the peri-urban region was dominated by agricultural activity, and land resources were converted into impervious surfaces. Although built-up area conversion is one of the indicators of economic development, but ecological imbalances, and food scarcity are great challenges against rapid urbanization. The water bodies decreased by 4.84 percent during the study period due to encroachment by dwellers of the city. However, all shrunk water bodies were located in the municipal area and played an important role in managing the overall environment of the Varanasi city. The barren land decreased by 82.41 percent between 1991 and 2022 because it is the least expensive land for buying and converting into built-up areas for settlements. Fallow land also decreased by 26.18 per cent but it has majorly converted into agricultural land. The vegetation cover shrunk during 1991-2011. The period between 2011 and 2022 witnessed a 12.5 percent increase in inclination toward social forestry, which can be attributed to a major initiative undertaken by the government and the changing perception of people.

Overall, the built-up area noted a high rate of expansion, and it covered 182.16 km^2 in 2022. In the central parts of the city, the horizontal as well as vertical sprawl was observed with dense concreted urban features. High land rent within the municipal area, holy nature, better connectivity, and availability of basic amenities are the main reasons behind the faster pace of urbanization in the VCDR. In consequence, the quality of the environment, urban morphology, and quality of life are declining. In the spatial context, changes in land use have been identified both on the outskirts of the urban region and in proximity to the central business

district. A decrease in the rate of land use transformation was noted on moving away from the CBD and other nuclei of the city. Other parts like Ramnagar town, Pt. Deendayal Upadhyay Nagar and Babatpur developed as satellite towns based on their urban mobility and land use dynamics. The urban expansion of these towns can prove advantageous for the Varanasi city as it has been grappling with the issue of overpopulation for the past few decades and these towns can be new topophila for upcoming migration streams in future time. Varanasi city has grown in the form of multiple axes due to highway expansion and better connectivity to newly established settlements. These facts help to understand the land use pattern and dynamics as well as the cultural and physical morphology of the Varanasi city. Hence, Monitoring land use dynamics through LULC mapping and assessment is one of the most efficient approaches to reducing urban sustainable vulnerability. The geographical information of various LULC classes and their transformation may assist Varanasi City in effective planning and policy to enhance carrying capacity and sustainability by demonstrating where, what, and how changes have happened in the city landscape.

CONCLUSION

The outcome of this study presents that the city is experiencing hyper-urbanization and rapid LULC transformation. Since 1991, the built-up area increased by five times, and other classes like agricultural land, fallow land, and barren land have declined rapidly. The focal points of transformation are within the municipality, nearer to the municipal boundary, and along the roads and railway lines. The fundamental and advanced infrastructural development, like major service centers, geographic location, and religious importance of the city, are the most attractive factors affecting land use alteration. So, proper land use planning for upcoming decades is needed to maintain the optimum land resource utilization, food security, and a healthy physical and social environment. This study has produced an important catalog on the dynamics of LULC and its transformation over the past three decades that can be used as a comprehensive spatial database for planning and policy-making to improve the carrying capacity of the city and bring environmental sustainability to the study area.

ACKNOWLEDGMENT

The authors would like to express their gratitude to USGS and the developers of the GEE web portal. We want to convey our sincere thanks to the University Grant Commission (India) for providing a fellowship as a Senior Research Fellowship. Author Atul K. Tiwari recieves this fellowship (Fellowship ID: 190520639704).

REFERENCES

Arévalo, P., Bullock, E.L., Woodcock, C.E. and Olofsson, P. 2020. A suite of tools for continuous land change monitoring in Google Earth Engine. Front. Clim., 2: 1-19. DOI: 10.3389/fclim.2020.576740

Baig, M.F., Mustafa, M.R.U., Baig, I., Takaijudin, H.B. and Zeshan, M.T. 2022. Assessment of Land Use Land Cover Changes and Future Predictions Using CA-ANN Simulation for Selangor, Malaysia. Water, 14(3): 402. DOI: 10.3390/w14030402

Cao, L.S., Xu, H. and Li, H. 2022. Effect of greening trees on thermal comfort of the pedestrian streets in hot summer and cold winter regions in China. Nat. Environ. Pollut. Technol., 21(4): 1543-1552. DOI: 10.46488/NEPT.2022.v21i04.007

Chandole, V. and Joshi, G.S. 2023. Case study of rainfall and temperature assessment through trend and homogeneity analyses in Vadodara and Chhotaudepur district of Gujarat State, India. Environ. Monit. Assess., 195(5): 561. DOI: 10.1007/s10661-023-11089-w

Chughtai, A.H., Abbasi, H. and Karas, I.R. 2021. A review on change detection method and accuracy assessment for land use land cover. Remote Sens. Appl. Soc. Environ., 22: 100482. DOI: 10.1016/j.rsase.2021.100482

Francis, T. 2012. Land-cover changes: A comparison of change detection techniques. Int. J. Remote Sens., November 2012, 37-41.

Geng, J., Xu, L., Wang, Y. and Tu, L. 2023. Study of land cover change in the city with the fastest economic growth in China (Hefei) from 2000 to 2020 based on Google Earth engine platform. Remote Sens., 15(6): 1604. DOI: 10.3390/rs15061604

Gomes, V.C.F., Queiroz, G.R. and Ferreira, K.R. 2020. An overview of platforms for big earth observation data management and analysis. Remote Sens., 12(8): 1-25. DOI: 10.3390/RS12081253

Gudex-Cross, D., Pontius, J. and Adams, A. 2017. Enhanced forest cover mapping using spectral unmixing and object-based classification of multi-temporal Landsat imagery. Remote Sens. Environ., 196: 193-204. DOI: 10.1016/j.rse.2017.05.006

Henits, L., Jürgens, C. and Mucsi, L. 2016. Seasonal multitemporal land-cover classification and change detection analysis of Bochum, Germany, using multitemporal Landsat TM data. Int. J. Remote Sens., 37(15): 3439-3454. DOI: 10.1080/01431161.2015.1125558

Hu, Y. and Hu, Y. 2019. Land cover changes and their driving mechanisms in Central Asia from 2001 to 2017 supported by Google Earth Engine. Remote Sens., 11(5): 554. DOI: 10.3390/rs11050554

Kim, C. 2016. Land use classification and land use change analysis using satellite images in Lombok Island, Indonesia. For. Sci. Technol., 12(4): 183-191. DOI: 10.1080/21580103.2016.1147498

Lu, Y., Chen, D., Jiang, Y. and Huang, H. rong. 2005. Study of dental caries prevalence in children of Yinchuan in China. West China J. Stomatol., 23(6): 502-504.

Mahmoud, A.S., Mezaal, M.R., Hameed, M.R. and Naje, A.S. 2022. A Framework for Improving Urban Land Cover Using Object and Pixel-Based Techniques via Remotely Sensed Data. Nat. Environ. Pollut. Technol., 21(5): 2189-2200. DOI: 10.46488/NEPT.2022.v21i05.013

Mishra, P.K., Rai, A. and Rai, S.C. 2020. Land use and land cover change detection using geospatial techniques in the Sikkim Himalaya, India. Egypt. J. Remote Sens. Space Sci., 23(2): 133-143. DOI: 10.1016/j.ejrs.2019.02.001

MohanRajan, S.N., Loganathan, A. and Manoharan, P. 2020. Survey on Land Use/Land Cover (LU/LC) change analysis in remote sensing and GIS environment: Techniques and Challenges. Environ. Sci. Pollut. Res., 27(24): 29900-29926. DOI: 10.1007/s11356-020-09091-7

Naikoo, M.W., Rihan, M., Shahfahad, Peer, A.H., Talukdar, S., Mallick, J., Ishtiaq, M. and Rahman, A. 2022. Analysis of peri-urban land use/land cover change and its drivers using geospatial techniques and geographically weighted regression. Environ. Sci. Pollut. Res., 012: 345. DOI: 10.1007/s11356-022-18853-4

Osman, T., Shaw, D. and Kenawy, E. 2018. An integrated land use change model to simulate and predict the future of the greater Cairo metropolitan region. J. Land Use Sci., 13(6): 565-584. DOI: 10.1080/1747423X.2019.1581849

Pal, A., Tiwari, A.K. and Kanchan, R. 2023. Slumscape through the prism of urban geomorphology: A Study of Vadodara City, India. Indian J. Spatial Sci., 14(2): 1-9

Pande, C.B. 2022. Land use/land cover and change detection mapping in Rahuri watershed area (MS), India, using the Google Earth engine and machine learning approach. Geocarto Int., 37(26): 13860-13880. DOI: 10.1080/10106049.2022.2086622

Pandey, P.C., Koutsias, N., Petropoulos, G.P., Srivastava, P.K. and Ben-Dor, E. 2021. Land use/land cover in view of earth observation: Data sources, input dimensions, and classifiers: A review of the state of the art. Geocarto Int., 36(9): 957-988. DOI: 10.1080/10106049.2019.1629647

Rwanga, S.S. and Ndambuki, J.M. 2017. Accuracy assessment of land use/land cover classification using remote sensing and GIS. Int. J. Geosci., 08(04): 611-622. DOI: 10.4236/ijg.2017.84033

Saravanan, S. and Abijith, D. 2022. Flood susceptibility mapping of Northeast coastal districts of Tamil Nadu India using multi-source geospatial data and Machine Learning techniques. Geocarto Int., 1: 1-30. DOI: 10.1080/10106049.2022.2096702

Shi, M., Wu, H., Fan, X., Jia, H., Dong, T., He, P., Baqa, M.F. and Jiang, P. 2021. Trade-offs and synergies of multiple ecosystem services for different land use scenarios in the Yili River Valley, china. Sustainability, 13(3): 1-15. DOI: 10.3390/su13031577

Shukla, A. and Jain, K. 2019. Modeling Urban Growth Trajectories and Spatiotemporal Pattern: A Case Study of Lucknow City, India. J. Indian Soc. Remote Sens., 47(1): 139-152. https://doi.org/10.1007/s12524-018-0880-1

Singh, S. and Talwar, R. 2013. Effects of topographic corrections on MODIS sensor satellite imagery of mountainous region. Sign. Process. Commun., 18: 455-460. https://doi.org/10.1109/ICSPCom.2013.6719833

Smiraglia, D., Ceccarelli, T., Bajocco, S., Salvati, L. and Perini, L. 2016. Linking trajectories of land change, land degradation processes, and ecosystem services. Environ. Res., 147: 590-600. https://doi.org/10.1016/j.envres.2015.11.030

Sobha, P. and Jose, J.P.A. 2023. Investigating the implications of transit-oriented land use development for a potential node in an urban metro for sustainability. Nat. Environ. Pollut. Technol., 22(2): 721-730. https://doi.org/10.46488/NEPT.2022.v21i04.007

Sudmanns, M., Tiede, D., Lang, S. and Baraldi, A. 2018. Semantic and syntactic interoperability in online processing of big Earth observation data. Int. J. Digital Earth, 11(1): 95-112. https://doi.org/10.1080/17538947.2017.1332112

Tiware, A. 2014. Urban sciences, big data, and India. Glob. J. Multidiscip. Stud., 3(12): 14-25.

Tyagi, A., Tiwari, R.K. and James, N. 2023. Mapping the landslide susceptibility considering future land-use land-cover scenario. Landslides, 20(1): 65-76. https://doi.org/10.1007/s10346-022-01968-7

Wagh, N.D. 2022. A review on atmospheric dispersion system for air pollutants integrated with gis in urban environment structures. Nat. Environ. Pollut. Technol., 21(4): 1553-1563. https://doi.org/10.46488/NEPT.2022.v21i04.008

ORCID DETAILS OF THE AUTHORS

Atul K. Tiwari: https://orcid.org/0000-0003-4944-4625
Anindita Pal: https://orcid.org/0000-0001-7839-1855
Rolee Kanchan: https://orcid.org/0000-0001-8773-4362